'Photogrammetric Week 01' D. Fritsch & R. Spiller, Eds. Wichmann Verlag, Heidelberg 2001.

Combining LIDAR and IfSAR: What can you expect?

BRYAN MERCER, Calgary

ABSTRACT

Three-dimensional mapping products in the form of DEMs (Digital Elevation Models) have become much more accessible in recent years, in part due to the implementation of LIDAR and IFSAR technologies. While there is considerable familiarity with one technology or the other, they are not often examined in terms of their mutually similar characteristics or equally those that are dissimilar. The purpose of this paper is to summarize those factors which will ultimately help to determine whether one technology or the other is appropriate for a particular application. We present two examples to illustrate and suggest that in many ways they can be viewed as complementary rather than competitive technologies.

1. INTRODUCTION

Airborne laser scanning altimetry, often referred to simply as LIDAR, has enjoyed explosive growth in the past three years. Although the entry cost is not trivial, the growth rate of users is about 25%/year (Flood, (1999)) with an estimated 60 or so systems in existence at this time. At the same time, interferometric SAR (IFSAR) has created wide interest both in its space-borne manifestations (repeat-pass ERS-1/2 and dual antenna SRTM missions) as well as the airborne implementations. In this paper, the focus will be on airborne rather than space-borne IFSAR as it creates a DEM product closer to that of LIDAR in terms of its three-dimensional 'detail'. Detail, in this context relates to vertical accuracy on the one hand, and to the horizontal sample spacing on the other. With both airborne technologies providing DEM products, the question is often 'which technology to use?'. In general terms, as shown below, IFSAR is more cost effective for large-area applications, while LIDAR may be appropriate for more detailed delineation of ground features in built-up or forested areas. Ultimately it depends upon the application and the economic value of the information derived as to which, if either, technology is the more appropriate. In section 2, aspects of the two technologies are summarized from the point of view of common or shared characteristics, and then from the perspective of dissimilarities. A generic set of LIDAR specifications is compared with those of the STAR-3*i* IFSAR system of Intermap Technologies and the general price/performance relationship is presented in section 3. Two examples illustrating performance in different contexts are provided in section 4.

2. TECHNICAL BACKGROUND

In the following discussion, we limit our remarks to the airborne implementations of IFSAR and LIDAR, although the principles (not the details) of their space-borne counter-parts are mostly the same. Because IFSAR is relatively less understood than the small-footprint scanning LIDAR systems (see for example the LIDAR reviews of Baltsavias (1999), and Wehr and Lohr (1999)), we provide, as background to the sections that follow, a very brief technical description of IFSAR. The purpose of the subsequent sections is to highlight both the similarities and differences of the two technologies from technical, operational and phenomenological points-of-view.

2.1. IFSAR Background

Detailed descriptions of the interferometric process can be found in the literature, (e.g. Goldstein et. al., (1988), Rodriguez and Martin (1992), Gray and Farris-Manning (1993)). The following

illustrates the principles from a geometric viewpoint. The geometry relevant to height extraction, ‘h’, is illustrated in Figure 1.
there will be a path-difference ‘δ’ between the two wave-fronts. The baseline angle ‘θ_b’ is obtainable from the aircraft inertial system, the aircraft height is known from DGPS and the distance from antenna to pixel is the radar slant range. Then it is simple trigonometry to compute the target height ‘h’ in terms of these quantities. The path-difference is measured indirectly from the phase difference between the wave-fronts as they are received sequentially at the two antennas . Because the phase difference can only be measured between 0 and 2π (modulo 2π), there is an absolute phase ambiguity that is normally resolved with the aid of coarse ground control and a “phase unwrapping” technique (e.g. Goldstein et al, 1988). Thus the extraction of elevation is performed on the “unwrapped” phase.

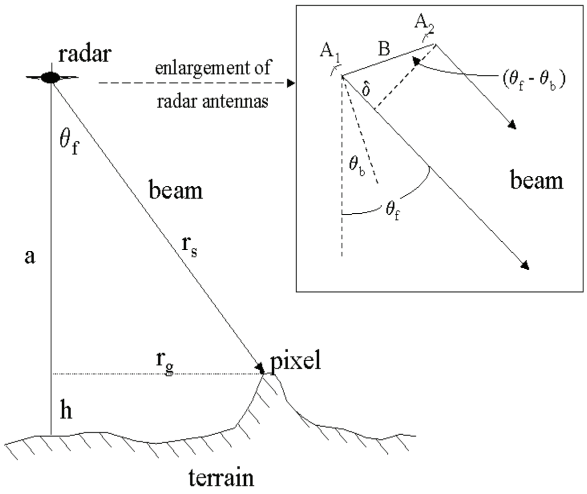

Figure 1. Schematic of Airborne IFSAR Geometry

2.1.1. STAR-3*i*

STAR-3*i* is an X-Band IFSAR, carried in a LearJet, and is owned and operated by Intermap Technologies Inc., Englewood, CO, USA. It was originally developed by ERIM and has been described by Sos et.al. (1994). It has been operated commercially since early 1997. Its basic operating characteristics are shown in table 1. In the following sections, although IFSAR is referred to in a generic sense, certain operational and price characteristic relate to STAR-3*i* specifically.

2.2. Shared Features of IFSAR and LIDAR

Airborne IFSAR and LIDAR share a number of common features. Ultimately they are both creating elevation models of the terrain from airborne platforms at superior levels of spatial detail (typically 1 – 5 meters sample spacing) and accuracy (typically 15 cm – 3 meters RMSE vertical). Some of the common features are noted below.

2.2.1. Active, Coherent Systems

They are both active systems, transmitting pulses and receiving the back-scattered returns. Both systems measure the 2-way time-delay from the transmitting element to the scattering elements and convert this to a range measurement. System parameters such as transmitted power and pulse repetition frequency impact system performance in each, although for different reasons. Additionally the coherent sources enable the focusing each is able to achieve, and in the case of IFSAR is fundamental to the interferometric aspect.

2.2.2. INS/GPS

They both require highly accurate attitude and positioning data in the form of on-board, coupled INS/GPS systems that are used to support the computation of the (x,y,z) coordinates of the scattering objects. In both systems (especially LIDAR) the positioning error, and particularly the roll angle error, are major factors in the system error budget.

2.2.3. Platform Dependence

The airborne platforms range from 'low and slow' to 'high and fast'. This choice has a major impact on performance (accuracy and sample density) and operating cost as well as schedule. Operating cost obviously converts into a major portion of the cost of the product to the user.

2.2.3.1. Flying Height

Both systems create a ground swath of data coverage, which is dependent upon the flying height of the platform. This of course directly affects the economics of the operation. Other quantities also scale with platform height. For example, in both cases the error in the INS-derived roll angle will be converted into an error in two of the recovered ground coordinates (x and z). In some cases certain entities are more sensitive in one system than the other. For instance, the IFSAR signal-to-noise ratio of the received pulse is altitude dependent and ultimately is one of the major components of the elevation error budget (e.g. Rodriguez and Martin, (1992)), while it is normally a minor component of the LIDAR error budget. On the other hand, the LIDAR spot diameter is altitude dependent while the IFSAR footprint is independent of altitude

2.2.3.2. Flying Speed

Flying speed impacts both operating cost and performance. The operational aspects are perhaps obvious. In the case of LIDAR, the major impact on performance relates to the along-track sample spacing, although with most systems there is a trade-off between along-track and cross-track spacing. Typically IFSAR is designed to operate within a broad window centered on a nominal operating speed. Within that window, there is no direct impact of speed on performance.

2.2.4. First Surface

Both systems respond to the first surface of contact (assuming it is a solid surface) which may be the bare terrain itself or objects such as buildings resting upon the terrain. The resulting model is usually referred to as a DSM (Digital Surface Model). A goal of users of both types of data is often to create a bald-earth DEM from the DSM (e.g. Wang, et al (2001)). The two systems respond differently to vegetation (see para 2.3.7 below).

2.3. Differences

Some of differences between the two systems and their impacts are summarized in the following.

2.3.1. Wavelength

IFSAR wavelengths (e.g. X-Band is ~3 cm) are such that they penetrate cloud, haze, etc. LIDAR wavelengths, as used in most mapping systems, are in the near IR (~1 nm), do not penetrate cloud, and are heavily absorbed by water.

2.3.2. Geometry

IFSAR is side-looking geometry – typical incidence angles range between 30 and 60 degrees. LIDAR viewing is centered on nadir, with symmetrical scans of varying magnitude (usually operator-controllable) depending on the manufacturer. Scan angles are often restricted within +/- 20 degrees of nadir, depending on application. The advantage of near-nadir viewing is that it limits problems associated with occlusion by buildings and other solid objects. The disadvantage is that for a given flying height it restricts the swath width, thereby increasing unit costs.

2.3.3. Spot Size and Sample Density

LIDAR samples are 'point-like' compared to IFSAR's 'area-like' elevation samples. The LIDAR illuminates a spot on the ground with diameter ranging from 10 – 100 cm, depending on altitude and other factors. The spot separation is usually 2 – 5 meters, depending on the various operating parameters, although for some applications, higher spot densities (sub-meter) are required and achieved. The resulting data set is an irregular or semi-regular grid of (x,y,z) coordinates. For visualization and other purposes, these are usually incorporated into a regular, gridded DEM using an interpolating package.

IFSAR, on the other hand, creates a regular grid of elevation samples directly. All the scattering elements within each of the contiguous resolution cells contributes to the observed elevation of that cell (Rodriguez and Martin, (1992)). The resulting DEM samples are therefore a result of integration rather than interpolation. In the case of STAR-3*i*, the interferogram has undergone some filtering in the upstream processing stage, so that the sample spacing at the output is usually 5 meters, which is twice the width of the fundamental resolution unit. All other factors being equal, a LIDAR DEM would look different than an IFSAR DEM in areas of rapid terrain change due to these interpolation versus integration factors.

2.3.4. Vertical Accuracy

There is nothing inherent in the design and operation of either LIDAR or IFSAR that precludes the achievement of accuracies at the 5-10 cm RMSE level. However 'normal' design and operation are a compromise between cost and requirement. There is a range of requirements and these are driven by different applications which usually are cost sensitive. Therefore to some degree, the quoted accuracies reflect the application requirements and price sensitivity.

LIDAR accuracies for 'normal' operations are usually between 15 and 50 cm RMSE. At the upper end of this error range, factors such as slope (Kraus, (2000)) and operational factors such as scan angle or altitude, are probably responsible. Referring to the lower end of the error range, it has been stated by one well known North American service provider that " 30 cm (RMSE) is relatively easy to achieve operationally; 15 cm is also achievable but with considerably more effort".

The STAR-3*i* IFSAR normally quotes nominal specifications for its GT3, GT2, or GT1 products of 3, 2 or 1 meter RMSE respectively. In moderate, vegetation free terrain, a GT1 product normally has an experimentally-determined error of about 60 cm RMSE over large areas (e.g. Sties et.al., (2000)). At flying altitude appropriate to GT1 (~20,000') acquisition, the relative elevation 'noise' of the system is about 30cm (1σ). Over larger areas (10's of km) the systematic or time varying errors raise the overall error to the ~60cm level previously noted. As this manuscript is being prepared, an upgrade to the STAR-3*i* system is about to commence the objective of which is to reduce that error while maintaining the flying altitude and swath.

It should be noted that vertical accuracy is often stated in ambiguous terms. It is becoming more clear that vendors and users alike would benefit from more clearly defined conditions under which the specification is valid. For instance, vertical accuracy should be defined with respect to unambiguous terrain conditions, by which we mean bare, unobstructed and relatively flat terrain as the 'base condition'. Moreover if both relative and systematic error content are to be addressed, the areal extent of the test should be appropriate (more than a single swath width, for example).

2.3.5. Coverage

There is nothing inherently limiting for either technology that would preclude large or small area acquisition. However, because of its wider swath and greater flying speeds, IFSAR acquisition is generally more appropriate for large area coverage. This is reflected both by price and acquisition rate comparison.

2.3.6. Image

A gray scale image is created simultaneously with the elevation data by IFSAR. Because of the inherent co-registration of the image and elevation pixels, the resulting products are ortho-rectified. The pixel size of the current version of STAR-3*i* is 2.5 meters with 4 'looks'. The latter term means that the image has been averaged down (x4) to reduce speckle.

LIDAR doesn't have an equivalent imaging capability, although some service providers have solved the problem by incorporating a digital camera in the same mount as the LIDAR with optics enabling overlapping coverage (e.g. Toth, (2000)). Some newer LIDAR systems utilize the intensity information available from the back-scattered beam, and although this is not a full image because of the limited spot size, it could be very useful for supporting editing operations.

2.3.7. Forest Canopy Response

Radar penetrates into forest canopy by an amount that is dependant upon the wavelength (longer wave-length, greater penetration), incidence angle and the characteristics of the forest (stem density, height, etc). The height returned by the IFSAR is an integrated response over the vertical extent of the canopy. In dense forest conditions, an X-Band IFSAR generally measures an 'effective' height that corresponds to the top half of the canopy, while at the other extreme, P-Band may be measuring near the forest floor. Currently there is considerable research under way attempting to quantify P-Band capability for bare-earth extraction beneath the canopy.

LIDAR scatters from foliage, but if there are any holes to the forest floor, a portion of the pulse may penetrate all the way through the canopy, and scatter from the true ground surface. Provided the pulse rate is high enough and the forest cover sufficiently 'porous', the ground can be sampled with adequate density, enabling a good representation of the terrain surface to be obtained. The penetration rate of course varies with forest and operating parameters. A significant problem is the determination of what is truly a ground point rather than the result of a scatterer higher up. This is particularly problematic when there is dense understory. Some lidars now measure multiple returns in order to improve discrimination of true ground points.

2.3.8. Availability

According to Flood (2000) there are likely to be about 60-70 LIDAR systems in use world-wide by mid-2001. On the other hand, at this time there are only two companies operating IFSAR systems commercially, with a third about to come into operation within a year (there are many more used for research and military purposes). This may reflect in part the higher entry cost and greater operational complexity of the IFSAR, as well as the fact that it tends to be used in large area acquisition situations compared to LIDAR.

2.4. Summary of Specifications

Parameter	IFSAR (STAR-3i)	LIDAR (Typical)
Operating Altitude	20,000' – 30,000'	1,000' – 6,000'
Operational Speed	750 km/hr	~200 km/hr
Depression Angles (nom.)	30 – 60 deg.	+/- 20 deg (35 max)
Swath Width (ground plane)	5 – 8 km	0.7 – 1km
Image Pixel Spacing	2.5 m	Separate camera ?
DEM Sample Spacing	2.5, 5, 10 m	3 - 5 m (0.5 min)
DEM Vertical Accuracy* Absolute (RMSE) Relative (1s)	 m** ~30 cm	 15 - 35 cm -
DEM Horizontal Accuracy	2.5 m***	0.5 - 1.0 m
Collection Rates**** Maximum (kmsq/hr) Typical (kmsq/hr)	 4.000 1.000	 ~200 ?

Notes:
* Moderate terrain, bare-earth
** GT1spec
*** Based on the accuracy of the accompanying ORI
**** Typical rates account for line lengths, turns, overlap, etc

Table 1: Comparison of Selected Operating Parameters

Some of the specifications and performance parameters of interest are shown in table 1. It should be noted that the 'typical' LIDAR system denoted here would be flying in a fixed wing aircraft and would be characteristic of a number of systems in use over the period 1998 – 2000. It is recognized that a number of new systems are becoming available with better performance at higher altitude, higher PRF and so forth. Similarly, this table is not representative of the very high PRF, low altitude LIDARs such as some of the helicopter-borne systems or the TopoSys system. Similarly, we show only one of the STAR-3*i* modes of operation and recognize that this will shortly be out of date due to a scheduled upgrade.

3. THE PRICE FACTOR

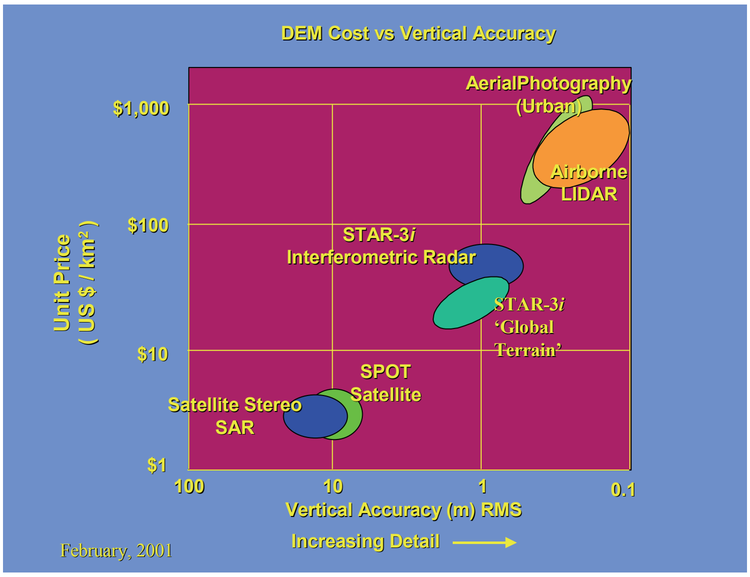

Figure 2: DEM Cost vs. Accuracy

Vertical accuracy and sample spacing (which together contribute to the perceived 'detail') are two of the major 'metrics' driving the cost, and the applicability, of DEM products. In figure 2, the unit price (US$/kmsq) of DEM products is shown as a function of vertical accuracy. For relative comparison, we show the relationship of satellite-based DEM products, STAR-3*i* IFSAR, and generic LIDAR. Because costs and specifications are often project-specific, there is a broad range for any data type, but the trend is clear. It should also be noted that price can be considerably reduced when data are available under licensing terms as shown in the comparison between STAR-3*i* project-based prices as contrasted by the 'Global-Terrain' prices which may be 2-3 times cheaper. In this case data rights are retained by the provider, the data reside in a data base, and the provider is at liberty to license the data to multiple users who therefore share the cost of acquisition and production. Of course this is a successful strategy only to the extent that the data base contains data in the user's area of interest.

4. TWO EXAMPLES

In the following, we present two comparisons of STAR-3*i* DEMs with those obtained by lidar. In both cases, the lidar was made available to the author as pre-filtered, bald-earth files of (x,y,z) data points. In both cases datum and projection conversions were required to bring both sets into a common frame of reference. For visualization purposes, the lidar points were interpolated into a regular grid using the 'Natural Neighbor' algorithm of the Vertical Mapper software package. In both cases the average lidar point spacing was similar to the 5 meter radar grid spacing. Statistical comparisons were usually done using the lidar points (x, y, z) and performing bi-linear interpolation on the radar data at the horizontal location of the lidar points.

4.1. Baden-Wurttemberg Example

The first example is for an area of mixed forest and agriculture in Germany. The terrain consists of rolling hills and valleys. The radar data were collected of the whole state of Baden-Wurttemberg by

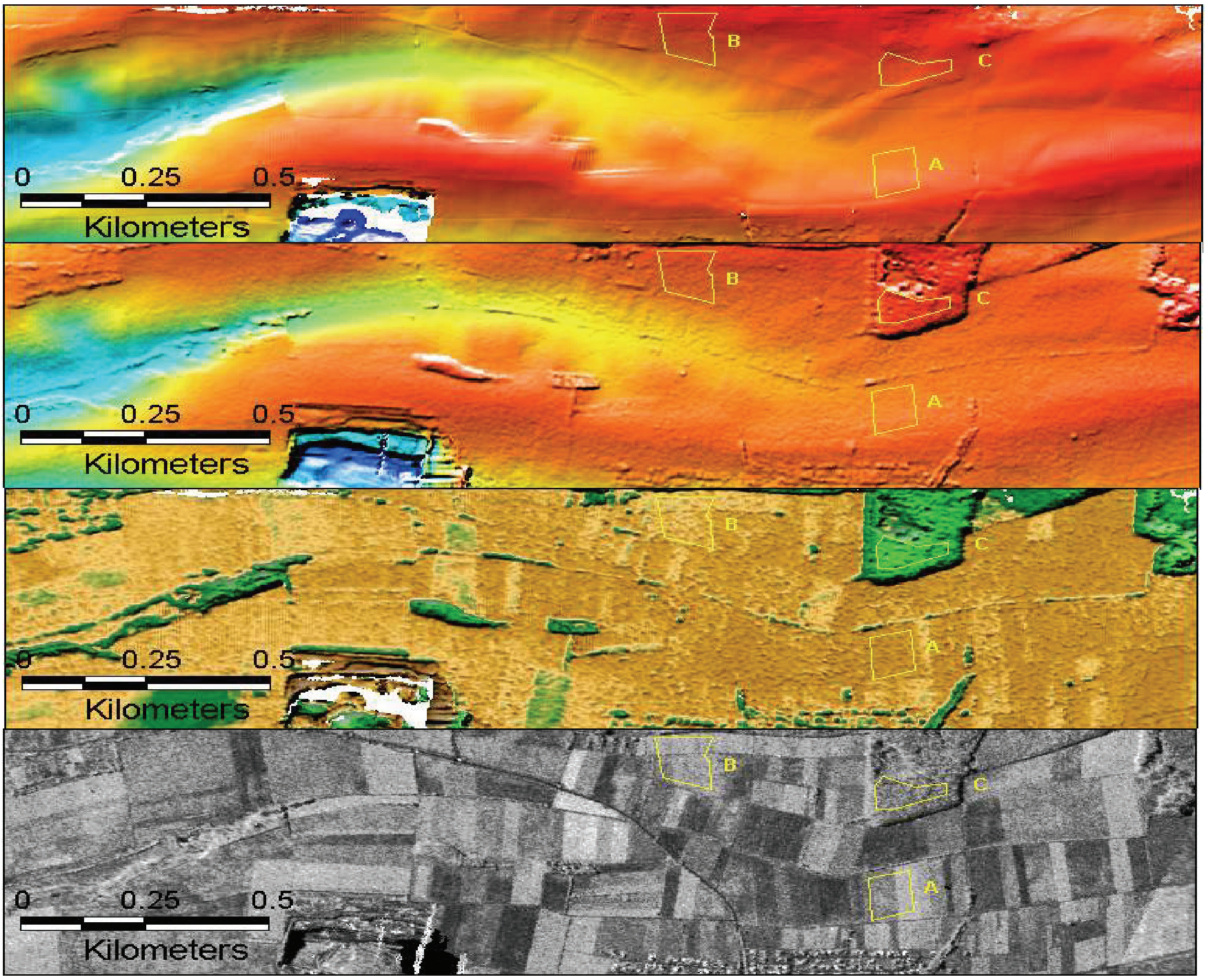

Figure 3: From top, Lidar DEM, IFSAR DSM, difference surface, radar ORRI.

the STAR-3i system in July, 1998. During this period, the vegetation was in full leaf and crops were well developed so the radar DSM would, of course, reflect the crops and forests as well as buildings and other objects. The state mapping agency (the LVA), had acquired lidar data for a sub-region of dimensions (10 km x 15 km) about 80 km NNW of Stuttgart. The data were acquired by Topscan in January, 1996 during leaf-off conditions. The residual vegetation and other objects had been removed by Topscan to create a bald-earth DEM.

The area presented here includes a strip about 0.8 km x 2.5 km in Northing and Easting respectively. The colorized DEMs from the Lidar and IFSAR are shown as the top two displays in figure 3 while the difference surface (IFSAR – Lidar) and the ortho-rectified radar image (ORRI) follow.

The terrain heights range from about 257 meters in the valley (blue) to about 303 meters on the highest ridge (red). As noted earlier, the Lidar DEM represents a bald-earth surface while the radar DEM includes the trees, crops and other objects above the ground. An interesting feature on the lower left side is a deep gravel quarry.

Areas depicted in white are due to under-sampling – that is, the absence of data within the 15 meter threshold placed on the surface interpolator. The difference surface shows the forest (and some buildings) in green, while the bald earth and low crops (< 2 meters) are in shades of cream and brown. The field conditions are quite evident in the ORRI. Forest and crop patterns as well as a village (lower right) are evident. Some of these characteristics are also evident in the difference surface. In particular, the forest, buildings, and some crop types are manifested by their height. It should be noted that the ORRI is a measurement of radar back-scatter and hence of roughness. Therefore, some low crops (e.g., cabbage) will appear rough and relatively bright in the ORRI but will not appear in the difference surface. On the other hand, crops such as corn appear in both.

Difference Surface Statistics STAR-3i minus Lidar			
Data Set		Mean (m)	Std Dev (m)
A	Bald Earth	-0,47	0,28
B	Crops	0,66	0,34
C	Forest	21,04	2,16

Table 2

Three polygons reference different surface conditions to be sampled statistically. Polygon ‘A’ is interpreted as bare-earth, ‘B’ is a crop (type unknown), and ‘C’ is forest. Mean and standard deviation for the difference surface is provided for each of them in Table 2. These results are consistent with those reported in Sties et.al. (2000).

The areas sampled are relatively small (~100m x 100m) and the resulting standard deviation for the bald earth area is about 28 cm, similar to that described as the ‘noise floor’ for the Red River example described in Mercer and Schnick (1999). The variability is slightly larger in area ‘B’, as would be expected in a crop covered region. The crop sample is about 1.1 meters higher than the bald-earth, and probably represents a scattering level lower than the visible surface. Sampling of bald-earth areas over the whole test area incorporates systematic errors of about 50 cm into the radar DEMs upon which the 30 cm noise floor is superposed. These systematic variations can be removed with control.

The other note of interest is the forested area which shows an effective mean height of 21 meters and a variability of about 2 meters. This is a reflection of the relative uniformity of the forest sample.

4.2. Morrison, CO Bald-Earth Example

The second example is of the Morrison, CO, USA quad. This 7.5' quad (~ 140 kmsq) is a test-site for various R&D projects sponsored by the USGS in Denver. The STAR-3*i* system of Intermap was contracted to acquire DSM and image products of the area as were two lidar companies. Lidar data from the 3Di (formerly Eaglescan) system, was made available to Intermap for test purposes. The data, in point form, was pre-filtered and edited by Eaglescan to create the ground points that were subsequently interpolated into a regular 5 meter grid for visualization and comparative purposes. The mean point spacing was about 5 meters. Statistical tests were performed using the point data to avoid additional interpolation errors, that become significant in steep terrain. The vertical accuracy specification was 15 cm RMSE and it was Intermap's intention to use it as wide-area 'truth' for comparative purposes. The lidar data were collected in June 1999 while the radar DSM was collected in October 1998 as a GT2 product. Normally GT2 precludes the use of ground control, but for this study some bulk normalization with respect to lidar was performed to remove vertical offsets in the radar DSM at the 1 meter level.

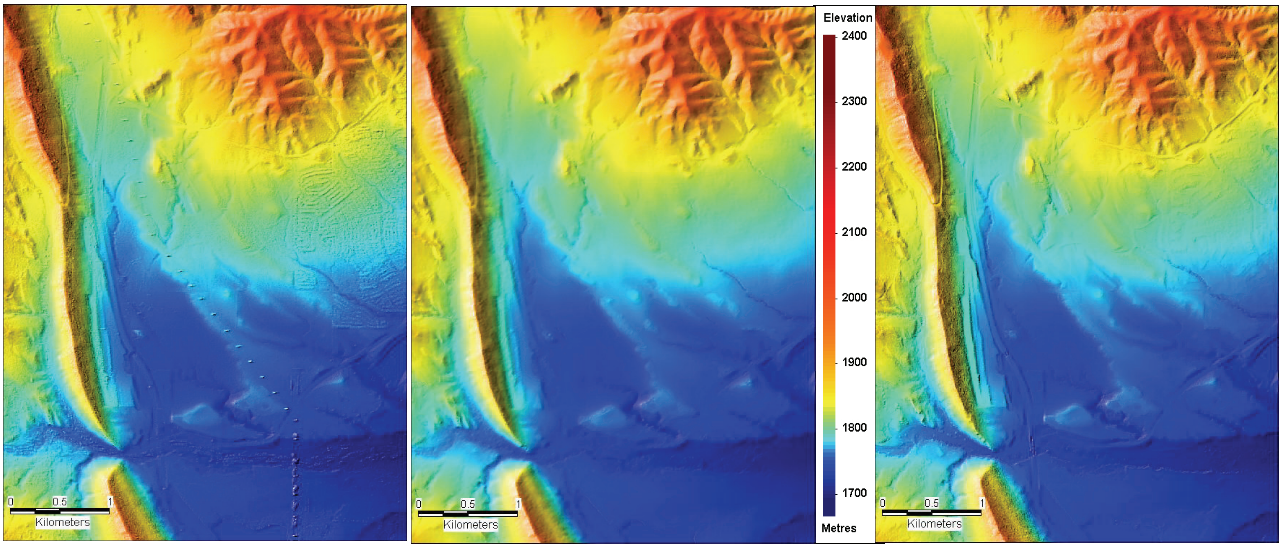

Figure 4: From left to right, STAR-3*i* DSM, STAR-3*i* Bald DEM, Lidar Bald-DEM

An automated algorithm was developed for extraction of the bald-earth DEM from the radar DSM (Wang, et al. (2001)). Specifically the objective was to remove buildings, trees and other objects from the DSM, in sparsely wooded areas in urban (non-core) and rural settings. A particular challenge was to retain the details of the topography. The Morrison quad is an excellent test site as it contains urban, and rural, treed and bare, variable topography from flat to very steep. A sub-set (`4km x 6 km) of the quad is displayed in figure 4. From left to right, the IFSAR DSM, the bald-earth DEM extracted from it, and the Lidar bald-earth DEM are shown. The urban area (center-right), power transmission pylons, and other objects are clearly manifested in the DSM. Equally clearly they are absent in the bald-earth DEM. Several types of comparative test were performed and the results of two of these are shown here.

The DSM for the quad as a whole is displayed in Figure 5. The polygons enclose relatively homogeneous sub-areas that are representative of five classes of interest. These include flat areas, bald areas, urban areas, Green Mountain (moderate mountainous), and the western mountains (steep mountainous). Difference statistics (Radar – Lidar) of the bald-earth DEMs were calculated for these classes, and are presented in figure 5. The 'bald' and 'flat' classes showed a ~55 cm RMSE difference which is characteristic of the wide area systematic noise of STAR-3*i*. The urban and

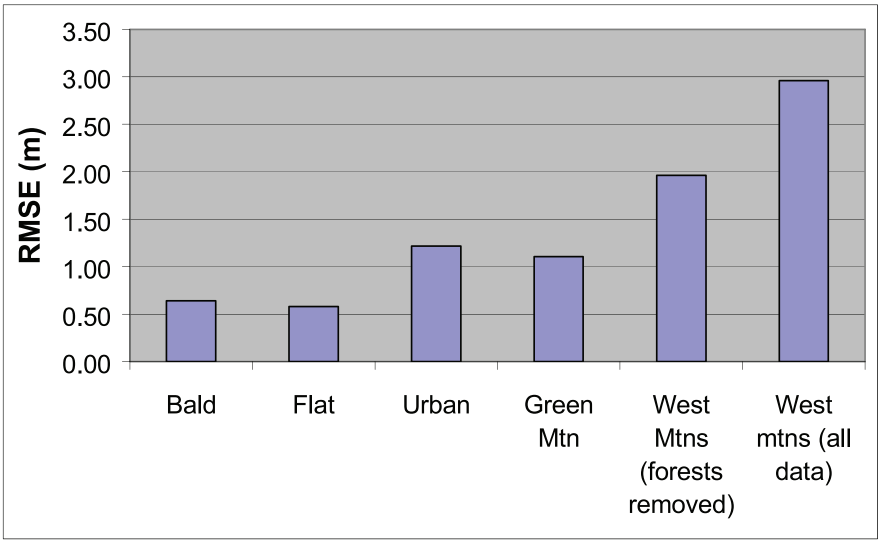

Figure 5: (Radar – Lidar) Bald-Earth DEM Difference Statistics

moderately mountainous statistics show differences of slightly over one meter which is probably distributed between the two systems. In the western mountains, there are substantial patches of forest covering about a third of the area, and the bald-earth algorithm will not handle these areas. Thus they are contributing to the total apparent difference. Based upon Ikonos imagery of then area, the large forest patches were masked and out of the calculations and the results show a difference in the remaining two thirds of the area to be about 2 meters RMSE. It is expected that the steep slopes are creating problems with both systems. A horizontal error in either system will translate into a slope-dependant vertical error. No independent ground control was available for further clarification.

An interesting qualitative comparison can be made by examining contours created from each of the bald-earth DEMs. In figure 6, three meter contours from each of the bald DEMs have been overlaid on the STAR-3*i* ORRI of a small sub-set (~2.25 km x 2.25 km) of the area previously shown in Figure 4 (note the power poles). The contours were generated identically and no additional contour smoothing was performed. The contours are very similar overall, with some differences apparent upon close inspection.

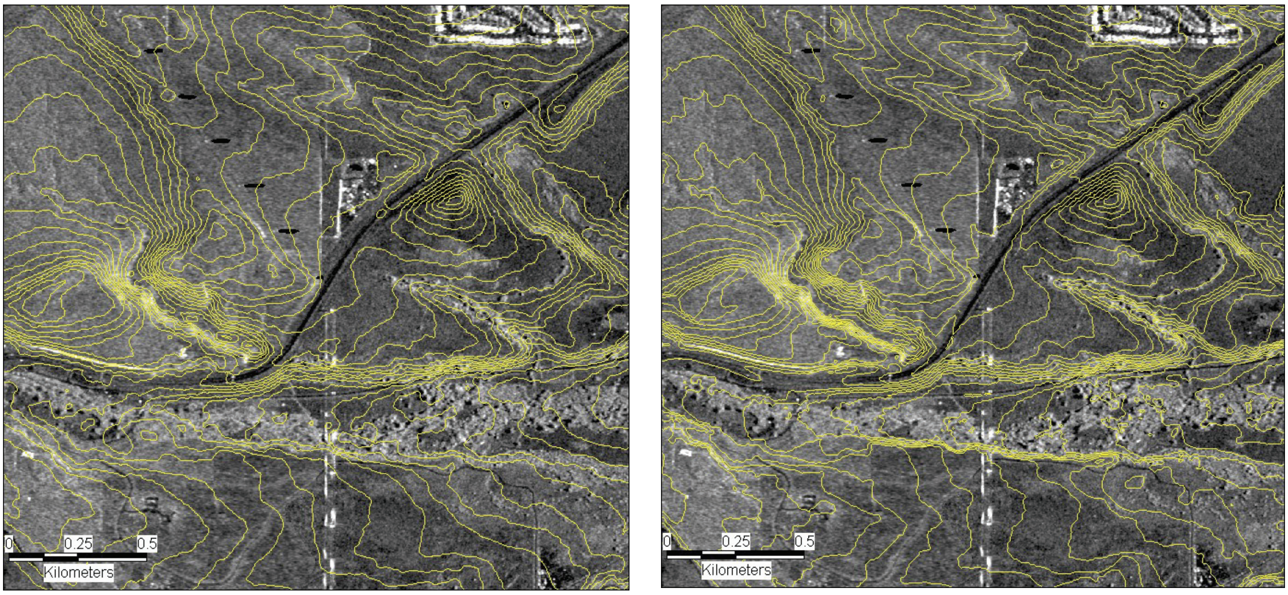

Figure 6: From left to right, 3 meter contours from (a) STAR-3*i* Bald-DEM, (b) Lidar Bald-DEM overlaid

5. CONCLUSIONS

A number of technical and operational similarities characterize these two active sensor systems, although there are equally important differences that are relevant to the specific application. As demonstrated, the price/performance is an important consideration. It would appear that in many applications the optimum strategy would be to combine the best attributes of both technologies. In sparsely-vegetated and non-core urban areas, IFSAR is very competitive for large area coverage, while the performance may e adequate for many applications. On the other hand LIDAR offers several advantages including better bald-earth DEM performance in many forest-cover situations, and better geometry for urban-core building delineation. Strategies that take advantage of these complementary factors are likely to be realized in the near future.

6. ACKNOWLEDGEMENTS

The author acknowledges with gratitude the work of Intermap colleagues and ex-colleagues for contributions to the examples shown here. Dr. David Box of Eaglescan provided the lidar data in the Morrison example, and the Landesvermessungsammt (LVA) of Baden-Wurttemberg provided the Topscan lidar data in that example as part of a data exchange.

7. REFERENCES

Baltsavias, E.P. (1999). Airborne laser scanning: existing systems and firms and other resources, Remote Sensing of Environment. Vol. 54, No. 2-3, pp. 164-198

Flood, Martin (1999). Commercial Development of Airborne Laser Altimetry. Proceedings of the ISPRS Workshop, La Jolla, CA, pp. 13-20.

Gray, Laurence A., and P.J. Farris-Manning, (1993). Repeat-Pass Interferometry with Airborne Synthetic Aperture Radar. IEEE Transactions on Geoscience and Remote Sensing. Vol. 31: Number 1, pp 180-191.

Goldstein, R.M., H.A. Zebker, and C. Werner, (1988). Satellite Radar Interferometry: two dimensional phase unwrapping. Radio Sci. Vol. 23: Number 4, pp 713-720.

Mercer, J. Bryan and Steve Schnick (1999). Comparison of DEMs from STAR-3i Interferometric SAR and Scanning Laser. Proceedings of the ISPRS Workshop, La Jolla, CA, pp. 127 - 134.

Sos, G. Tim, Herbert W. Klimach and Gray F. Adams (1994). High Performance Interferometric SAR Description and Capabilities. Tenth ERIM Thematic Conference on Geologic Remote Sensing, San Antonio, Texas, Vol. II, pp. 637-649

Sties, Manfred, Susanne Kruger, J. Bryan Mercer and S. Schnick (2000), Comparison of Digital Elevation Data from Airborne Laser and Interferometric SAR Systems. Proceedings of the XIXth Congress of the ISPRS , Amsterdam, Vol XXXIII, Part B3, P866-873.

Toth, Charles K., Sandra Berning, James Leonard and Dorota A. Grejner-Brzezinska (2001). Integration of Lidar Data With Simultaneously Acquired Digital Imagery. Proceedings of ASPRS 2001, St. Louis, Missouri

Wehr, A. and U.Lohr (1999) Airborne laser scanning - an introduction and Overview. ISPRS Journal of Photogrammetry and Remote Sensing, Vol. 54, No. 2-3, pp. 68-82.